Impact of the MEC Location in Transport Networks on the Capacity of 5G to Support V2X Services

Baldomero Coll-Perales[1], M. Carmen Lucas-Estañ[1], Chang-Heng Wang[2], Javier Gozalvez[1], Takayuki Shimizu[2], Sergei Avedisov[2], Miguel Sepulcre[1], Takamasa Higuchi[2], Bin Cheng[2], Akihiko Yamamuro[3], Onur Altintas[2]

[1]Uwicore laboratory, Universidad Miguel Hernandez de Elche, Elche (Alicante), Spain.
[2]InfoTech Labs, Toyota Motor North America R&D, Mountain View, CA, U.S.A.
[3]Toyota Motor Corporation, Japan
[1]{bcoll, m.lucas, j.gozalvez, msepulcre}@umh.es
[2,3]{chang-heng.wang, takayuki.shimizu, sergei.avedisov, takamasa.higuchi, bin.cheng, akihiko.yamamuro, onur.altintas}@toyota.com

Abstract— **5G networks have been designed to support advanced and demanding services in critical verticals or industries such as connected and automated driving. Supporting advanced Vehicle to Everything (V2X) services may require installing Multi-access/Mobile Edge Computing (MEC) platforms that reduce the latency and the traffic load on the transport and core networks by deploying services and computing resources closer to the edge of networks. 3GPP and ETSI indicate that the MEC can be installed on the transport network at different locations between the base station and the core network. The specific MEC location has important technical and business implications. This has also strong implications on the dimensioning of the link capacity of the 5G transport network. In this context, this paper studies the link capacity demand that supporting advanced V2X services generate on the 5G transport network depending on the MEC location in the transport network. The paper considers gradual 5G deployments going from 5G Non-Stand-Alone (NSA) networks relying on the 4G Evolved Packet Core (EPC) network to 5G Stand-Alone (SA) deployments with a 5G Core Network. In addition, the paper evaluates the processing capabilities necessary to install V2X Application Servers (AS) at MEC nodes. The results show that it can be challenging for 5G NSA networks to support scaling V2X services, while 5G SA networks will require non-negligible link capacities and significant MEC processing and computing power as MEC nodes are located closer to the core network and the vehicular traffic increases. These results call for careful dimensioning of the transport network and an optimized MEC location to support V2X services without starving other 5G services.**

Keywords—5G, MEC, Mobile Edge Computing, transport network, V2X, connected automated vehicles.

I. INTRODUCTION

5G introduces novel technologies and mechanisms to support a wide range of services with requirements grouped into three QoS categories: Ultra-Reliable Low Latency Communications (URLLC), enhanced Mobile BroadBand (eMBB), and Massive Internet of Things (MIoT). The advanced capabilities of 5G to provide low latency, high bandwidth and massive communications result in part from its New Radio (NR) interface. 5G NR incorporates new slot formats, modulation and coding schemes, and flexible numerologies, among others, that significantly reduce the latency, and increase the reliability and flexibility of 5G networks. Multi-access/Mobile Edge Computing (MEC) is another fundamental technology to facilitate the support of these services as it brings computing and storage resources closer to the end users and reduces the latency. 5G networks have raised expectations on the possibility to

support (safety critical) connected automated V2X applications, including some that traditionally are supported using Vehicle-to-Vehicle (V2V) communications. In this case, 5G would replace the direct V2V communication with a connection between the vehicles through the cellular network, i.e. Vehicle-to-Network-to-Vehicle (V2N2V). Proof-of-concept trials have shown promising end-to-end results of V2N2N [1][2]. These trials generally rely on the use of MEC platforms that reduce the latency by processing the V2X applications closer to the vehicle. At the same time, these field trials are mainly conducted with a limited number of vehicles and are based on a dedicated infrastructure. Therefore, the question remains on whether 5G networks can scale and support the strict requirements of critical V2X services to a larger number of users without starving or compromising other 5G services.

3GPP and ETSI have identified MEC as a key 5G technology to support advanced and demanding connected automated V2X services. Installing the MEC on the transport network has important technical and business implications depending on where it is located in between the base station and the core network. Locating the MEC closer to the base station reduces the latency and the processing capabilities required for MEC nodes since they serve a smaller number of users. However, it requires a large number of MEC nodes for ubiquitous service provisioning. On the other hand, locating the MEC nodes closer to the core network reduces the number of MEC nodes necessary to support a large number of users but increases the latency and the network traffic load on the 5G transport network. The specific MEC location has also strong implications on the dimensioning of the link capacity of the 5G transport network. This is because of the hierarchical architecture of the transport network which includes different traffic aggregation levels. Therefore, a MEC location closer to the base station reduces the traffic load and link capacity requirements of the transport network links compared with locating it closer to the core network.

In this context, this paper studies the tradeoffs of the MEC location in the transport network. Since 5G deployment has just started, the study considers a gradual evolution towards 5G deployment going from a 5G Non-Stand-Alone (NSA), that relies on 4G transport networks and the Evolved Packet Core (EPC), to 5G Stand-Alone (SA) deployments that are supported by 5G transport networks and the 5G Core (5GC). For each deployment scenario, this study first derives the link capacity demand that supporting advanced V2X services generates on the transport network. To this aim, this paper models the transport

network as a queueing system and derives the capacity of the transport network's links that needs to be reserved to support the traffic load generated by V2X services. The paper also evaluates the processing capabilities necessary to deploy V2X Application Servers (AS) at MEC nodes to support the V2X services. The conducted evaluation shows the challenges that 5G NSA networks can experience to support advanced V2X services as the traffic load grows. 5G SA can better support the V2X service traffic demand, but the required link capacities and MEC processing capabilities are non-negligible as MEC nodes are located closer to the core network. These link capacity demands need to be carefully estimated and considered in the dimensioning of 5G transport networks so that other 5G services are not negatively affected. The rest of this paper is organized as follows: Section II introduces the considered transport network architecture and scenario, and Section III shows the potential locations where MECs can be installed. Section IV and V describe the modeling of the transport network and V2X AS that is used to find out their stability conditions. Section VI shows the evaluation conditions and the obtained results, and Section VII summarizes the main conclusions.

II. TRANSPORT NETWORK ARCHITECTURE AND SCENARIO

This work uses the transport network architecture recommended by the ITU-T Study Group 15 [3] as a reference. This architecture is generally utilized by 4G networks and is being evolved to meet the 5G requirements. However, operators may deploy their networks according to their own scenarios and needs so the transport network architecture presented in [3] and illustrated in Fig. 1.a should be taken as a reference example. The transport network connects the radio interface to the core network, and has a hierarchical architecture as shown in Fig. 1.a. The figure uses the general term Active Antenna Unit (AAU) to refer to the base station or infrastructure element in the radio interface following [3]. The transport network comprises two segments or domains named access and aggregation. The transport network reference technical specifications commonly refer to these segments or domains as metro-edge and metro-aggregation, respectively, whereas 3GPP specifications refer to fronthaul and midhaul, respectively. We will follow the more general convention of access and aggregation in this paper.

Following [3], we consider a transport network scenario where the AAUs are connected to the nodes of the access domain via point-to-point links. In particular, each node of the access domain is connected to 6 AAUs via point-to-point links. Following the nomenclature utilized in [4], we will refer to the nodes of the access domain that are connected to the AAUs as M1. In the reference scenario, 6 of these M1 nodes connected in a ring topology form an access ring. Therefore, each access ring serves a total of 36 AAUs. Then, M2 nodes operate as gateways between the access and aggregation domains. Each M2 node serves as a gateway to 4 access rings, and each M2 node serves a total of 144 (i.e. 36x4) AAUs. An aggregation ring is made of 6 M2 nodes. Finally, M3 nodes serve as gateways between the aggregation domain and the core network. In particular, the reference architecture indicates that an M3 node provides gateway capabilities to 2 aggregation rings, so each M3 serves a total of 1728 AAUs (144x6x2). Fig. 1.a shows that M1 and M2 are connected following a ring topology. This ring configuration is considered to be at the electrical level while at the logical level they are connected point-to-point to their corresponding gateways [4][5]. In this context, M1 nodes are directly connected to M2 nodes, and M2 nodes to M3 nodes. This point-to-point topology in the access and aggregation rings brings important benefits since packets are only queued once at the gateway level, while a ring topology requires queueing packets at every intermediate node towards the gateway node.

Designing the transport network requires adequate dimensioning of the link capacities or link speeds to support the traffic demand and service requirements [4][6]. For example, the study reported in [4] derives the link capacity of the transport network architecture of [3] necessary to support a mixture of flows generated by eMBB, URLLC and MIoT services. The study identifies necessary speeds of 10 Gb/s for the AAU-M1 links, 300 Gb/s for the M1-M2 links, and 6 Tb/s for the M2-M3 links. [7] shows an example of a commercial transport network for 4G that is characterized by 1 Gb/s in the AAU-M1 links (in [7] the AAU is the 4G's eNode B), and 10 Gb/s and 100 Gb/s links in the access and aggregation rings, respectively. In [6], the ITU recommendations establish scalable link speeds determined by the number of {10, 25, 50, 100, 200, 400} Gb/s interfaces introduced in the access and aggregation domains. For example, [6] establishes that the transport network link speeds to support 5G requirements include: N_1 x {10, 100, 200} Gb/s in the M1-M2 links and N_2 x {100, 200} in the M2-M3 links (when connected point-to-point), where N_1 and N_2 are the number of links necessary to support the services requirements. In line with ITU recommendations, the Next-Generation Optical transport network Forum (NGOF) reports in [8] an example of the evolution of the transport network link speeds to support the requirements of 4G LTE, an early deployment of 5G that reutilizes the 4G transport network and a mature 5G deployment that increases the transport network link speeds. This evolution reported in [8] coincides with the evolution considered in 3GPP from 5G Non-Stand Alone (NSA) to 5G SA networks [5][9].

III. MEC LOCATIONS AT THE TRANSPORT NETWORK

Several organizations like 3GPP, ETSI, ITU and 5G-PPP identify the importance of installing MECs to reduce the latency and the load on the transport network [10]. There are multiple options available to physically locate the MEC nodes. A feasible option for the physical MEC location is a network aggregation point within the transport network [11]. ETSI refers to the installation of MEC on the transport network as "*bump in the wire*" and it defines it as "*all scenarios in which the MEC platform installation point ranges in locations between the base station itself and the mobile core network*" [12].

A key aspect for exploiting the benefits of MECs is the ability to route the traffic to/from the MEC applications. In 4G networks, steering traffic to/from MEC applications is achieved by configuring the MEC's local DNS (Domain Name System) and the MEC host's data plane. The local breakout functionality (i.e., the ability to route traffic over a close gateway) can also facilitate locating MEC in the transport network. However, the local breakout capabilities are limited in 4G [11] compared to 5G. Expanded functionalities in 5G include (see details of these functionalities in clause 5.13 of [10]): 1) User Plane Function (UPF) local exposure to perform routing and traffic steering to/from the MEC location; 2) service and session continuity to
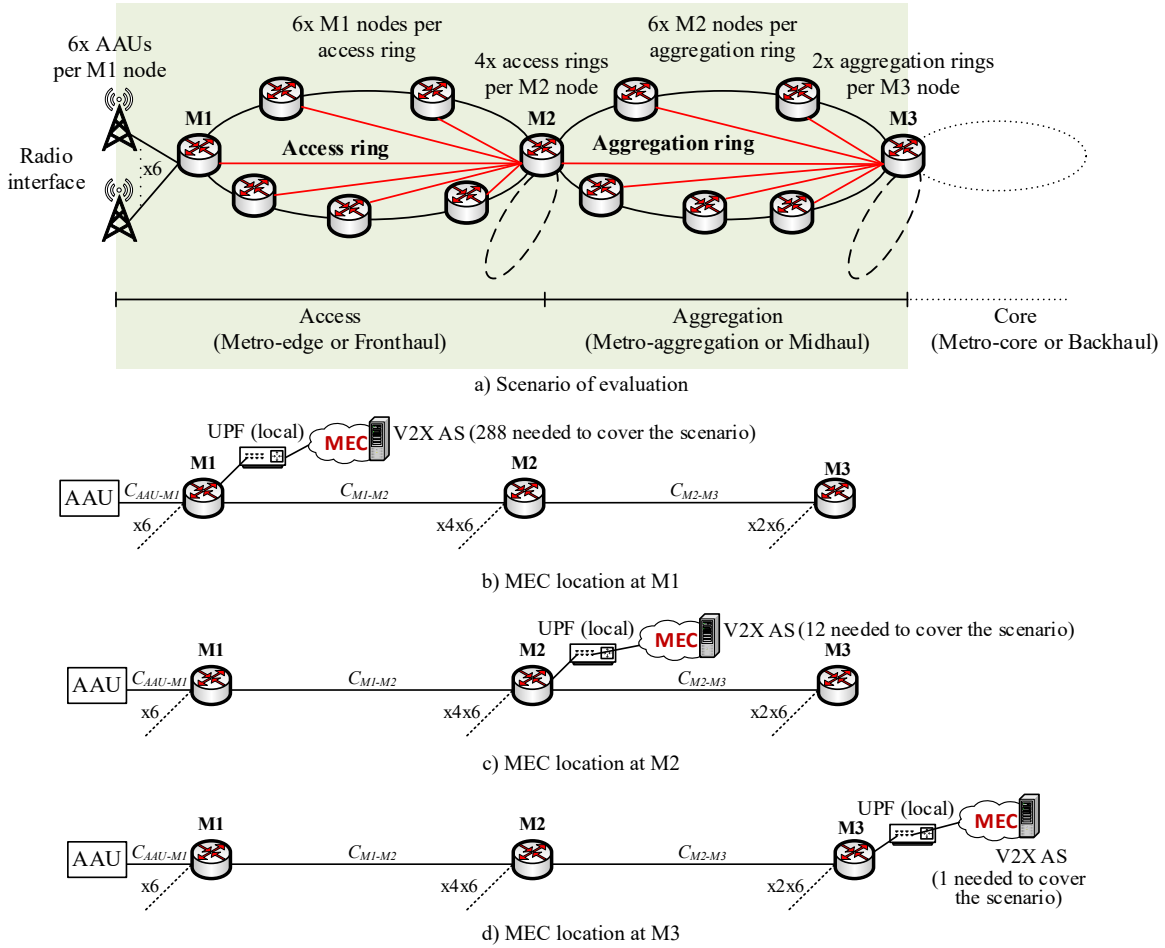
Fig. 1. Reference transport network architecture and transport network scenarios for different MEC locations.

support the user mobility; 3) support to MECs located at the edge from the 5G core network. Without loss of generality, we indicate that the traffic steering and routing functionalities are implemented in the UPF.

A. MEC at the access domain interface in M1

Fig.1.b represents the first scenario where the MEC is co-located with the transport network node that interfaces the access domain (i.e., at the node M1). Following Section II, the AS hosted in this MEC serves a total of 6 AAUs and it necessitates a total of 288 MEC nodes to cover the scenario. Traffic generated and addressed to the AS hosted in the MEC follows the following path in the uplink: 1) packets correctly received at the AAU are forwarded to the M1 node; 2) UPF's traffic steering and routing functions filter out the packets matching the steered traffic and direct them towards the AS hosted in the MEC. In the downlink, the reverse path is followed starting at the AS that connects to the M1 through the UPF. M1 forwards the packets towards the AAU. The links that intervene in the processing of V2X services in this MEC location include then the AAU-M1, M1-UPF and UPF-AS links.

B. MEC at the aggregation domain interface in M2

The second scenario installs the MEC at the transport network node that interfaces the aggregation domain, i.e., at the

node M2. This is represented in Fig. 1.c where the AS at the MEC is in charge of serving a total of 144 AAUs considering the transport network reference scenario described in Section II. Locating the MEC at the M2 node requires then only 12 MEC nodes to cover the scenario. Traffic generated and addressed to the AS hosted in the MEC follows the following path in the uplink: 1) packets that are correctly received at the AAU are routed at the access domain by the M1 node towards the aggregation domain; 2) the M2 node passes the traffic to the UPF node that performs the traffic filter matching to steer the appropriate traffic towards the AS hosted in the MEC. Packets follow the reverse path in the downlink, i.e., from the AS the packets reach the M2 node through the UPF, and from the M2 the packets are forwarded to M1 to finally reach the AAU. The links participating in this second MEC location include the AAU-M1, M1-M2, M2-UPF and UPF-AS links.

C. MEC at the core interface in M3

We consider a third scenario where the MEC is co-located with the transport network node that interfaces the core, i.e., the node M3. This is illustrated in Fig. 1.d. In this case, the AS hosted in the MEC serves all AAUs present in the considered transport network reference scenario, i.e., a total of 1728 AAUs. A single MEC node is also required since the M3 node is at the highest aggregation level of the transport network. Traffic

generated and addressed to the AS hosted in the MEC follow the following path in the uplink: AAU-M1, M1-M2 and M2-M3 links. The UPF's traffic steering and routing functions forward then the packets towards the AS hosted in the MEC. The reverse path is followed in the downlink. In this third MEC location, the following links participate in the routing of packets: AAU-M1, M1-M2, M2-M3, M3-UPF and UPF-AS.

IV. TRANSPORT NETWORK MODELING

We propose modeling the transport network scenario described in Section II as a queueing system in order to analyze its dimensioning based on the envisioned MEC locations and V2X services to support. Following the study reported in [4], each node of the transport network is modeled as an M/M/1 queue. In M/M/1 queues, each node is represented with a single server that processes arrivals that are determined by a Poisson process, and the service time of the node follows an exponential distribution. M/M/1 queues also assume that the server buffer has an infinite capacity.

A. General concepts

We first show how to model a general network node in order to introduce important concepts that are later utilized for our complete transport network modeling. We first describe how to model the packet aggregation in the uplink transport path and the packet splitting in the downlink transport network path given the hierarchical structure of the transport network architecture. To this aim, we utilize the general schematic of a node in a queueing system that is illustrated in Fig. 2. Each node of a queueing system is characterized by the parameters λ and μ that represent the arrival rate of traffic to the node, and the service rate or departure rate of traffic from the node. In Fig. 2.a, the node has N input links, and each of these links is characterized by an arrival rate $\lambda_{in, i}$, $i = 1, …, N$. Due to the properties of Poisson processes, the overall or aggregate arrival traffic to the node is also a Poisson process, with aggregate arrival rate $\lambda_{agg} = \sum_{i=1}^{N} \lambda_{in, i}$. This aggregation process occurs in the uplink path of our architecture, e.g., M1 aggregates the traffic of 6 AAUs. Fig. 2.b represents the case where a node has M output links. The traffic that is processed at each output link is a portion of the packet arrival rate λ. If we refer to p_j as the portion of λ that is addressed to the output link j ($j = 1…, M$), the arrival traffic that the node has to dispatch through the output link j is a Poisson process, with $\lambda_{out,j} = p_j \cdot \lambda$. Note that all packets that arrive at the node have to be dispatched, so the condition $\sum_{j=1}^{M} p_j = 1$ must be satisfied. This process of splitting traffic takes place at the downlink, e.g., the downlink traffic arriving at M1 has to be
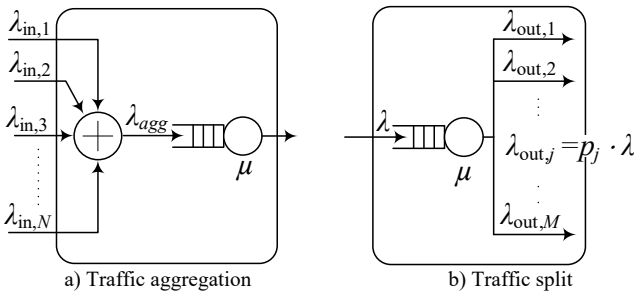
routed to 6 AAUs. Without loss of generality, we assume an even traffic split in our analysis, i.e., $p_j = 1/M$, $j = 1, …, M$.

Finally, it is also important to introduce the concept of node stability in queueing systems. The stability of a node shows whether it can process all received packets or not. Nodes characterized by infinite buffers, like in M/M/1 queues, are not stable if the traffic arrival rate is higher than the service rate or departure rate. This is the case because the buffer backlog would increase to infinity and there would be packets that never depart the node in a finite amount of time. The stability of a node is computed as:

$$\rho_j < 1, \tag{1}$$

where ρ is the node utilization or proportion of time that the link is busy transmitting packets and is defined as $\rho = \lambda/\mu$.

B. Modeling

We focus on modeling the transport network with the MEC located at M3 since this case includes all links of the transport network, and therefore covers the two other scenarios that locate the MEC at M1 or M2.

1) Uplink transport network path

Fig. 3 shows a graphical representation of the transport network with the MEC at M3 as a queueing system. The system illustrates the uplink transport network path, and each node is characterized by λ and μ (measured in packets/s). The link between two nodes of the queueing system is characterized by C that represents the link capacity (measured in bits/s).

At an AAU node, the arrival rate of traffic is determined by the traffic generated by the UEs in the cell. Let's consider that there are N_{UE} UEs in the cell that generate packets of B bytes at an average rate of T packets/s. Then, $\lambda_{AAU,UL}$ and $\mu_{AAU,UL}$ can be computed as:

$$\lambda_{AAU,UL} = N_{UE} \cdot T, \tag{2}$$
$$\mu_{AAU, UL} = \alpha_{AAU-M1} \cdot C_{AAU-M1} / B. \tag{3}$$

In (3), C_{AAU-M1} is the link capacity between the nodes AAU and M1, and α_{AAU-M1} represents the fraction of this link capacity allocated to support the traffic of a specific service in the uplink path. We can then define the node's utilization $\rho_{AAU,UL}$ as:

$$\rho_{AAU,UL} = \lambda_{AAU,UL} / \mu_{AAU,UL} = \frac{N_{UE} \cdot T \cdot B}{\alpha_{AAU-M1} \cdot C_{AAU-M1}}. \tag{4}$$

If we consider the queueing system has no losses, the traffic at the output of a node is the same as its input rate λ. The arrival rate of traffic to the node M1 can then be computed as $\lambda_{M1,UL} = \sum_{i=1}^{6} \lambda_{AAU,UL,i}$, where $\lambda_{AAU,UL,i}$ is the arrival rate of traffic to AAU connected to the M1 node following the scenario presented in Section II. If we assume the same traffic under each AAU, then $\lambda_{M1,UL}$ can be computed as $\lambda_{M1,UL} = 6 \cdot \lambda_{AAU,UL}$. The service rate of the M1 node can then be computed as $\mu_{M1,UL} = \alpha_{M1-M2} \cdot C_{M1-M2} / B$, where C_{M1-M2} is the link capacity between the nodes M1 and M2, and α_{M1-M2} represents the fraction of this link capacity allocated to support the traffic of a specific service. Note that α_{AAU-M1} and α_{M1-M2} can take different values. Similarly, C_{AAU-M1} and C_{M1-M2} can also be different. We can then compute the utilization of M1 as:

$$\rho_{M1,UL} = \lambda_{M1,UL} / \mu_{M1,UL} = \frac{6 \cdot \lambda_{AAU,UL}}{\alpha_{M1-M2} \cdot C_{M1-M2}/B} = \frac{6 \cdot N_{UE} \cdot T \cdot B}{\alpha_{M1-M2} \cdot C_{M1-M2}}. \tag{5}$$

Fig. 2. General schematic of a node in a queueuing system.

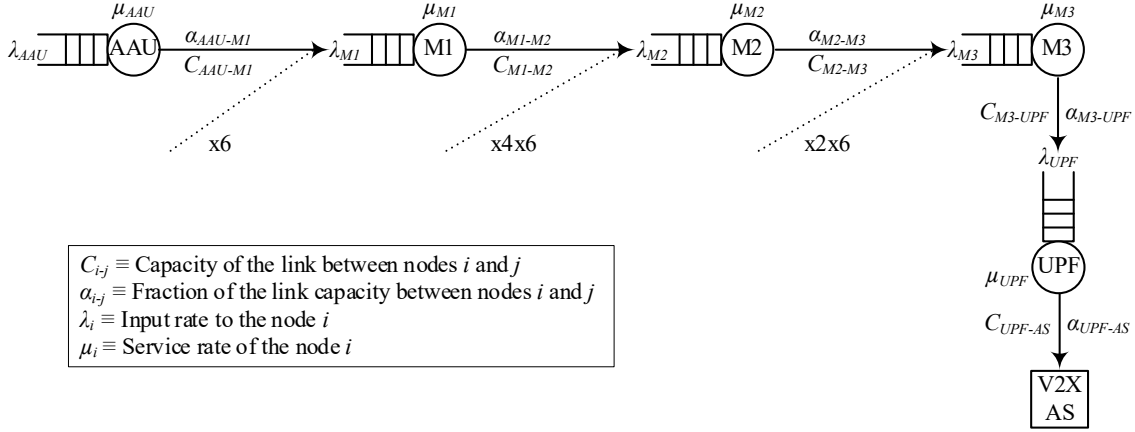a) Traffic aggregation

b) Traffic split

Fig. 3. Representation of the transport network with the MEC at M3 as a queuing system.

Following the same process as for M1, we can compute the arrival rate of traffic to M2 as $\lambda_{M2,UL} = 6 \cdot 4 \cdot \lambda_{M1,UL}$. $\lambda_{M2,UL}$ is derived considering that each M2 node serves as a gateway to 4 access rings, and that each access ring comprises 6 M1 nodes as described in Section II. The service rate of the M2 node is computed as $\mu_{M2,UL} = \alpha_{M2-M3} \cdot C_{M2-M3} / B$. C_{M2-M3} is the link capacity between the nodes M2 and M3, and α_{M2-M3} represents the fraction of this link capacity allocated to support the traffic of a specific service. Then, the utilization of the node M2 is computed as:

$$\rho_{M2,UL} = \lambda_{M2,UL} / \mu_{M2,UL} = \frac{24 \cdot \lambda_{M1,UL}}{\alpha_{M2-M3} \cdot C_{M2-M3}/B} = \frac{144 \cdot N_{UE} \cdot T \cdot B}{\alpha_{M2-M3} \cdot C_{M2-M3}}. \quad (6)$$

The M3 node serves as a gateway to 2 aggregation rings, and each aggregation ring encompasses 6 M2 nodes (see Section II). The arrival rate of traffic to M3 can be computed as $\lambda_{M3,UL} = 6 \cdot 2 \cdot \lambda_{M2,UL}$. Similarly, the service rate of the M3 node can be computed as $\mu_{M3,UL} = \alpha_{M3-UPF} \cdot C_{M3-UPF} / B$. Note that C_{M3-UPF} represents the capacity of the link between M3 and the UPF considering that the traffic at M3 is steered towards the UPF node. α_{M3-UPF} represents the fraction of C_{M3-UPF} allocated to support the traffic of a specific service. The utilization of the M3 node is then estimated as:

$$\rho_{M3,UL} = \lambda_{M3,UL} / \mu_{M3,UL} = \frac{12 \cdot \lambda_{M2,UL}}{\alpha_{M3-UPF} \cdot C_{M3-UPF}/B} = \frac{1728 \cdot N_{UE} \cdot T \cdot B}{\alpha_{M3-UPF} \cdot C_{M3-UPF}}. \quad (7)$$

To complete the model, we must also characterize the UPF node and its connection to the (V2X) AS. Since there is no traffic aggregation nor traffic split from the node M3 to the (V2X) AS, the arrival rate of traffic to the UPF and (V2X) AS node coincides with the output rate of the M3 node. This can be expressed as $\lambda_{UPF,UL} = \lambda_{AS,UL} = \lambda_{M3,UL}$.

2) Downlink transport network path
The downlink transport network path starts at the (V2X) AS which generates $\lambda_{AS,DL}$ packets/s based on the service type and characteristics. The downlink arrival rate of traffic to the UPF is equal to $\lambda_{AS,DL}$ since there is no traffic split in this node.

The traffic coming from the UPF node is split at the M3 node towards the two aggregation rings in the downlink transport network path, and each of these aggregation rings comprise 6 M2 nodes. Therefore, the arrival rate of traffic to M3 that is sent to each M2 node is expressed as $\lambda_{M3,DL} = \lambda_{UPF,DL} / 12$. The M3 node's service rate in the downlink is $\mu_{M3,DL} = \alpha_{M3-M2} \cdot C_{M2-M3} /$

B. We maintain the same notation for the link capacity as in the uplink transport network path (i.e., C_{M2-M3}) but use α_{M3-M2} to distinguish the fraction of this link capacity that is allocated to support V2X traffic in the downlink. In fact, downlink and uplink traffic may be asymmetric while the capacity of the link is independent of the uplink or downlink directions. Then, the utilization of the M3 node in the downlink is:

$$\rho_{M3,DL} = \lambda_{M3,DL} / \mu_{M3,DL} = (\lambda_{AS,DL} \cdot B) / (12 \cdot \alpha_{M3-M2} \cdot C_{M2-M3}). \quad (8)$$

Considering both uplink and downlink, the fraction of the total link capacity C_{M2-M3} that is allocated to support the traffic of a specific service is:

$$\Lambda_{M2-M3} = \alpha_{M2-M3} + \alpha_{M3-M2}. \quad (9)$$

The node M2 also routes the traffic coming from the node M3 towards a node M1 in the downlink transport network path. Since our scenario has 4 access rings connected to each M2 node, and each access ring comprises 6 M1 nodes, the arrival rate of traffic to M2 in the downlink can be computed as $\lambda_{M2,DL} = \lambda_{M3,DL} / 24$, the service rate as $\mu_{M2,DL} = \alpha_{M2-M1} \cdot C_{M1-M2} / B$, and the node M2's utilization as:

$$\rho_{M2,DL} = \lambda_{M2,DL} / \mu_{M2,DL} = (\lambda_{AS,DL} \cdot B) / (288 \cdot \alpha_{M2-M1} \cdot C_{M1-M2}). \quad (10)$$

Therefore, the total fraction of the link capacity C_{M1-M2} that is allocated to support the traffic of a specific service is computed as:

$$\Lambda_{M1-M2} = \alpha_{M1-M2} + \alpha_{M2-M1}. \quad (11)$$

Finally, since the node M1 serves 6 different AUUs, the arrival rate of traffic to M1 that is split towards each AAU is $\lambda_{M1,DL} = \lambda_{M2,DL} / 6$. The M1 service rate is expressed as $\mu_{M1,DL} = \alpha_{M1-AAU} \cdot C_{AAU-M1} / B$, and the M1 node utilization is equal to:

$$\rho_{M1,DL} = \lambda_{M1,DL} / \mu_{M1,DL} = (\lambda_{AS,DL} \cdot B) / (1728 \cdot \alpha_{M1-AAU} \cdot C_{AAU-M1}). \quad (12)$$

The total fraction of the link capacity C_{M1-M2} that is allocated to support the traffic of a specific service is computed as:

$$\Lambda_{AAU-M1} = \alpha_{AAU-M1} + \alpha_{M1-AAU}. \quad (13)$$

V. V2X APPLICATION SERVER

The location of the MEC has strong implications on the network load it will have to process, and hence on the capabilities necessary for the V2X Application Server (AS). Dimensioning the processing power of the V2X AS must also

consider the V2X services it provides support to. For example, some V2X services may require that the AS processes some data, while others may just require the V2X AS to act as a forwarder, e.g., when replacing direct V2V links with V2N2V connections via the cellular network. In this study we consider the V2X AS act as a forwarder. Therefore, the output rate of traffic from the V2X AS can be expressed as $\lambda_{AS,DL} = n \cdot \lambda_{AS,UL}$, where n is the number of copies of the packet received at the V2X AS in the uplink that are forwarded in the downlink. For a scenario in which the AS hosted in a MEC forwards uplink V2X traffic in the downlink, Intel estimates in [13] the processing time at the V2X AS as:

$$l_{AS} = \eta \cdot B \cdot \theta / F, \tag{14}$$

where F is the processing capacity of the V2X AS (measured in cycles/s), B is the packet size, and η is the number of processed packets. The study in [13] considers that the received V2X packets require θ cycles/bit for processing. In [13], the authors model θ using a continuous uniform distribution $U(100, 300)$[1]. η depends on the time window established to process packets. We consider that the time window is set to the radio transmission time interval (e.g., 1ms-subframe in 4G or {0.25, 0.5, 1}ms-slot in 5G NR sub-6 GHz) that is denoted by t_{tt}. The arrival rate of packets to the V2X AS follows a Poisson distribution with mean $\lambda_{AS,UL}$ packets/s. We can then derive the average number of received packets in t_{tt} seconds as $\eta_{tt} = \lambda_{AS,UL} \cdot t_{tt}$. In order to ensure stability conditions at the V2X AS, it shall pursue $l_{AS} \leq t_{tt}$.

VI. EVALUATION

A. Evaluation scenario

We model a highway scenario of 6 lanes per direction with 80 vehicles/km/lane. The density of vehicles in a cell is computed using the distance between cells (or inter-site distance, ISD) that is set to 1732 m following 3GPP's reference highway deployment scenario [3GPP TR 38.913 V15.0.0 (2018-06) – Clause 6.1.8]. There are then in total more than 1650 vehicles in each cell. All cells have the same density of vehicles. The evaluation does not focus on a particular advanced V2X service. Instead, we consider that vehicles in the cells generate V2X packets of B= {300, 600} bytes [14]. Packets are generated following a Poisson distribution with mean T= {100, 50, 20} ms [14]. The packets are routed towards the V2X AS through the transport network in the uplink, and we consider that the V2X AS just forwards to the downlink the packets received in the uplink. We consider two forwarding scenarios. In the first scenario we assume that we can forward packets in the downlink using broadcast transmissions. However, broadcast is not yet supported in Rel. 15/16 5G NR, so we consider a second scenario where the V2X AS creates n=6 copies of each received V2X packet. The copies are forwarded towards the same cell where the originating vehicle is located as if they were transmitted to 6 neighboring vehicles.

Table I reports the capacity of the links between the nodes AAU and M1, M1 and M2, and M2 and M3 for the 4G and 5G transport network deployments that have been evaluated in this study. This information has been obtained from [7] for a commercial 4G transport network (commercial 4G), [4] for the ITU's 5G transport network (ITU 5G), and [8] for NGOF's early and mature 5G transport networks (early 5G and mature 5G).

TABLE I. LINK CAPACITIES FOR REFERENCE 4G AND 5G TRANSPORT NETWORK DEPLOYMENTS

| Transport network deployment	AAU-M1	M1-M2	M2-M3
Commercial 4G [7]	1 Gb/s	10 Gb/s	100 Gb/s
ITU 5G [4]	10 Gb/s	300 Gb/s	6 Tb/s
Early 5G [8]	10 Gb/s	200 Gb/s	1.6 Tb/s
Mature 5G [8]	25 Gb/s	500 Gb/s	4.6 Tb/s

B. Link capacity

Fig. 4 shows the minimum fraction of the link capacity (Λ) that needs to be allocated to the links between the nodes AAU and M1 (Fig. 4.a), M1 and M2 (Fig. 4.b), and M2 and M3 (Fig. 4.c) to support the traffic of the V2X service. Λ is computed for each of these links considering the fraction of the link capacity necessary in the uplink and downlink as shown in (13), (11) and (9), respectively. Λ is reported in Fig. 4 as a function of the network traffic load generated by each vehicle (or UE) that is computed as B/T. The results in Fig. 4 correspond to the scenario where 5G supports broadcast downlink transmissions, while Fig. 5 shows the results for the scenario where the V2X AS creates 6 copies of each V2X packet. Results are reported in Figs. 4 and 5 for the four transport network reference deployments (see Table II).

Locating the MEC at the M1 node only requires using part of the link capacity between the nodes AAU and M1 since the traffic is routed at the node M1 towards the V2X AS. Then, the results reported in Fig. 4.a show that locating the MEC at M1 of the commercial 4G transport network requires reserving at least 8% of the link capacity between the nodes AAU and M1 for the V2X service when the network traffic load per vehicle is just 24 Kbits/s. When this load increases to 240 Kbits/s, supporting the V2X service requires 80% of the commercial 4G link capacity between AAU and M1. Locating the MEC at M2 uses the links between the nodes AAU and M1, and between the nodes M1 and M2. Similarly, locating the MEC at the M3 node utilizes the links between the nodes AAU and M1, M1 and M2, and M2 and M3. Fig. 4 shows that when we locate the MEC at M3, supporting the V2X service when each vehicle generates a load of 240 Kbits/s requires using 80%, 48% and 116% of the link capacity of each of these links. This shows that the link between the nodes M2 and M3 in the commercial 4G transport network is a bottleneck for locating the MEC at M3. Fig. 5 shows that the commercial 4G transport network is also challenged to support the traffic of the V2X service under many of the evaluated traffic loads when the V2X AS creates 6 copies of each received V2X packet. For example, when the MEC is located at the node M1, the link between the nodes AAU and M1 becomes a bottleneck when the network traffic load generated per vehicle is equal or higher than 96 Kbits/s. Note that the link between the nodes
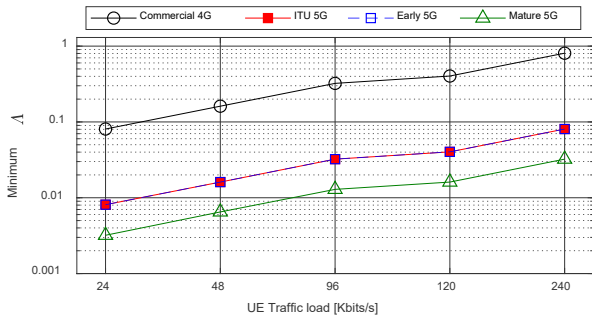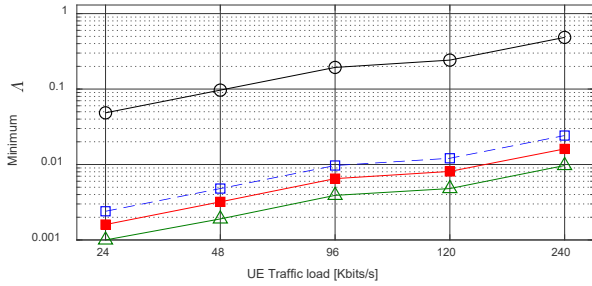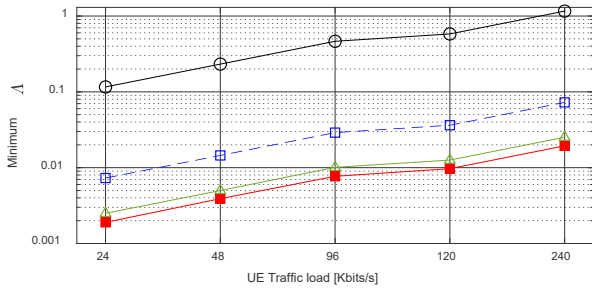

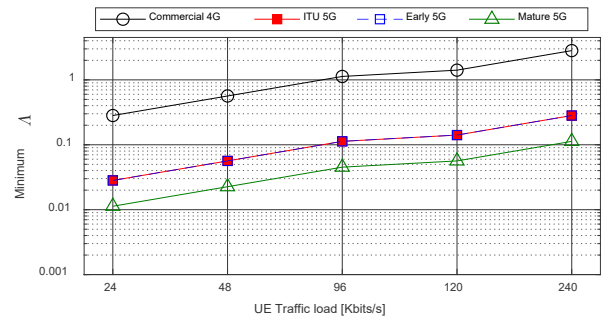
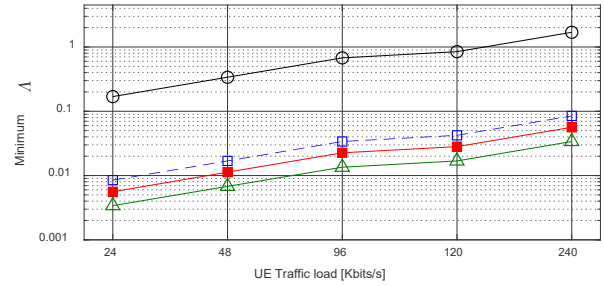Fig. 4. Minimum fraction of the link capacity necessary to support the traffic of the V2X service (scenario: broadcast downlink).

Fig. 5. Minimum fraction of the link capacity necessary to support the traffic of the V2X service (scenario: 6 copies in the downlink).

AAU and M1 is also the bottleneck when the MEC is located at M2 and M3 since the V2X traffic needs to pass first through this link to reach M2 and M3. In general, Figs. 4 and 5 show that the commercial 4G transport network is challenged to support the V2X service as the traffic load per vehicle increases. This also represents a challenge for 5G NSA to support scaling V2X services since 5G NSA also relies on 4G transport networks.
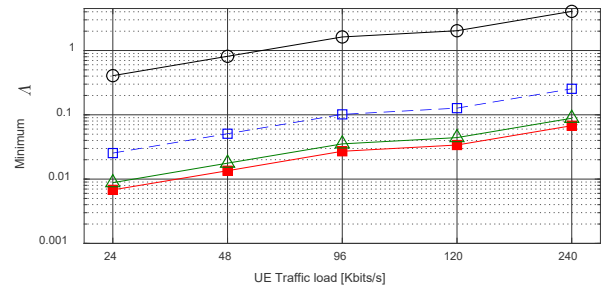
5G transport networks (i.e., ITU 5G, early 5G and mature 5G; see Table I) offer higher link capacities and reduce the value of Λ that is necessary to support the traffic of the V2X service for all possible locations of the MEC compared to the commercial 4G transport network (see Figs. 4 and 5). For example, when the MEC is located at M1 of the ITU 5G transport network, supporting the V2X service only requires 0.8% of the link capacity between the nodes AAU and M1 when each vehicle generates 24 Kbits/s compared to 8% for the commercial 4G transport network. The required link capacity increases to 8% for the link between the nodes AAU and M1 of the ITU 5G transport network when the network traffic load

generated by each vehicle increases to 240 Kbits/s. Scaling the network traffic load in Fig. 5 also increases the minimum fraction of the link capacities of the 5G transport networks necessary to support the traffic of the V2X service. For example, locating the MEC at the M3 node of the early 5G transport network results in that 28%, 8% and 25% of the link capacities between the nodes AAU and M1, M1 and M2, and M2 and M3, respectively, are necessary to support the V2X service when vehicles generate 240 Kbits/s of network traffic load each. On the other hand, the mature 5G transport network reduces the necessary link capacities to 11%, 3% and 8%, respectively, in the same scenario. Fig. 5 shows that for all 5G transport networks the highest fraction of the link capacities necessary to support the traffic of the V2X service is in the link between AAU and M1. This is important to be highlighted since the V2X traffic passes through this link under all possible locations of the MEC in the transport network. In this context, these results show that 5G transport networks should be carefully dimensioned to ensure the network can scale to support more V2X services and other non-V2X services considering the location of the MEC.

C. MEC processing capabilities

This section elaborates on the processing capabilities necessary to deploy the V2X AS at MEC nodes located at different nodes of the transport network. To this aim, we use the features of an Intel Xeon Gold 6252N processor that is typically used in MEC platforms as a reference [15]. This processor includes 24 independent cores, 48 threads of execution, and a maximum core frequency of 3.6 GHz. We have then computed the number of processors needed to process the V2X packets that arrive to the V2X AS in less than t_{tt} so that packets do not backlog and to ensure the V2X AS stability. This number is reported in Table II and is computed considering the Intel Xeon Gold 6252N specifications and (14). Table II shows that the location of the MEC on the transport network has a significant impact on the number of processors needed at each MEC node. This number considerably increases as MEC nodes are closer to the core network. While the increased number of processors is a disadvantage for MECs located closer to the core network, the advantage is that the total number of MEC nodes required is lower as it has been shown in Section III.

Next, we use the MEC platform reported by Intel in [16] that includes 96 Intel Xeon Gold 6252N processors as a reference. We then derive the average percentage of packets that are added to the queue of the V2X AS because they cannot be processed in less than t_{tt}. Packets are only added to the queue when the location of the MEC requires V2X AS with more than 96 processors. This is the case when the MEC is located at M3 close to the core network (see Table II). In all these scenarios the V2X AS queue is not stable. On average, the queue length is larger as the network traffic load generated by each vehicle increases; from 40.5% to 88.1% of packets are queued when the traffic load increases from 48 Kbits/s to 240 Kbits/s. These results demonstrate that an optimized dimensioning of the MEC is necessary depending on the location of MEC nodes on the transport network, the network load and the characteristics of the V2X services to be supported.

TABLE II.   MINIMUM NUMBER OF PROCESSORS NECESSARY TO ENSURE STABILITY AT THE V2X AS.

	UE traffic load				
	24 Kbits/s	48 Kbits/s	96 Kbits/s	120 Kbits/s	240 Kbits/s
MEC @ M1	1	1	2	2	3
MEC @ M2	7	14	34	27	68
MEC @ M3	81	162	404	323	807

VII. CONCLUSIONS

5G networks introduce technologies that are expected to support advanced safety critical services for connected automated driving. This includes the use of MEC platforms that reduce the latency by locating the processing closer to the edge and the vehicles. MEC platforms can be hosted at different locations of the transport network. This paper has analyzed the link capacities of the transport network necessary to support the traffic of V2X services depending on the location of the MEC. The MEC platforms may host V2X Application Servers (AS). The location of the MEC on the transport network has also strong implications on the required MEC processing power. The results obtained show that 4G transport networks cannot support V2X services as the network load increases. 5G transport networks can better address the traffic load generated by

advanced V2X services. However, non-negligible capacities of the 5G transport network links are required, especially when 5G does not support downlink broadcast transmissions. This can compromise the capacity of 5G to simultaneously support a variety of (V2X and non-V2X) services if networks are not properly dimensioned. The results also show that the MEC nodes require significant power and processing capabilities as they are deployed closer to core network in order to ensure the stability of the V2X AS.

REFERENCES

[1] K. Serizawa, M. Mikami, K. Moto and H. Yoshino, "Field Trial Activities on 5G NR V2V Direct Communication Towards Application to Truck Platooning", IEEE VTC2019-Fall, Honolulu, HI, USA, 2019, doi: 10.1109/VTCFall.2019.8891260.

[2] 5GAA, "5GAA live demos show C-V2X as a market reality", 5GAA press release, November 2019. Available online at [last accessed in Nov. 2020]: https://5gaa.org/wp-content/uploads/2019/11/5GAA-OFFICIAL-Press-Release_Turin-2019.pdf.

[3] ITU-T, "Consideration on 5G transport network reference architecture and bandwidth requirements", ITU-T Study Group 15, Contribution 0462, Feb. 2018.

[4] L. Cominardi, L. M. Contreras, C. J. Bcrnardos and I. Berberana, "Understanding QoS Applicability in 5G Transport Networks," IEEE BMSB, Valencia, Spain, 2018, doi: 10.1109/BMSB.2018.8436847.

[5] ITU-T, "Transport network support of IMT-2020/5G", Technical Report ITU-T GSTR-TN5G, Oct. 2018.

[6] ITU-T, "Application of optical transport netowrk; Recommendations to 5G transport", ITU-T G-series Recommendations – Supplement 67, Jul. 2019.

[7] H. Li, "5G Transport Network Requirements, Architecture and Key Technologies", ITU-T's workshops and seminars, Oct. 2017. Available online at [last accessed in Nov. 2020]: https://www.itu.int/en/ITU-T/Workshops-and-Seminars/20171016/Documents/2.%20Han%20Li.pdf

[8] Next-Generation Optical transport network Forum (NGOF), "5G-Oriented OTN Technology", Whitepaper, Mar. 2018.

[9] 3GPP TR 38.912, v15.0.0, "Study on New Radio (NR) access technology", Jul. 2018.

[10] 3GPP TS 23.501, v16.6.0, "System architecture for the 5G System (5GS)", Sept. 2020.

[11] ETSI, "MEC in 5G networks", White Paper No. 28, Jun. 2018. Available online at [last accessed in Nov. 2020]: https://portal.etsi.org/TB-SiteMap/MEC/MEC-White-Papers.

[12] ETSI, "MEC Deployments in 4G and Evolution Towards 5G", White Paper No. 24, Feb. 2018. Available online at [last accessed in Nov. 2020]: https://portal.etsi.org/TB-SiteMap/MEC/MEC-White-Papers.

[13] M. Emara, M. C. Filippou and D. Sabella, "MEC-Assisted End-to-End Latency Evaluations for C-V2X Communications", IEEE EuCNC, Ljubljana, Slovenia, 2018, doi: 10.1109/EuCNC.2018.8442825.

[14] M.C. Lucas-Estañ, et al., "On the Scalability of the 5G RAN to Support Advanced V2X Services", IEEE VNC 2020.

[15] Intel Official Web Site [las accessed in Nov. 2020]: https://ark.intel.com/content/www/us/en/ark/products/193951/intel-xeon-gold-6252n-processor-35-75m-cache-2-30-ghz.html.

[16] Intel, "Case Study of Scaled-Up SKT 5G MEC Reference Architecture", White Paper, Jun, 2020. Available online at [last accessed in Nov. 2020]: https://www.intel.com/content/dam/www/public/us/en/documents/white-papers/case-study-of-scaled-up-skt-5g-mec-reference-architecture.pdf